Research Square

Preprints are preliminary reports that have not undergone peer review.
They should not be considered conclusive, used to inform clinical practice,
or referenced by the media as validated information.

Spectrum and Determinants of Calcification Patterns in Uterine Fibroids: A CT-Based Retrospective Analysis

HUSAM VEHBI

wehbihusam@gmail.com

Sağlık Bilimleri Üniversitesi

serhat Kaya

Sağlık Bilimleri Üniversitesi

Gökay Kaan Sandalci

Sağlık Bilimleri Üniversitesi

Maide Yığıt

Sağlık Bilimleri Üniversitesi

Research Article

Keywords: Uterine fibroids, Leiomyoma, Calcification, Computed tomography, Pelvic imaging, Lesion size

Posted Date: July 25th, 2026

DOI: https://doi.org/10.21203/rs.3.rs-10034037/v1

License: This work is licensed under a Creative Commons Attribution 4.0 International License.
Read Full License

Additional Declarations: No competing interests reported.

Abstract

Purpose

To assess the spectrum of calcification patterns in uterine fibroids using computed tomography (CT) and identify their associations with lesion size, anatomical location, and margin characteristics in a Turkish population.

Methods

In this retrospective observational study, 140 women aged ≥ 30 years with CT-confirmed calcified uterine fibroids were examined at a tertiary care hospital between January 2020 and December 2025. A non-probability consecutive sampling method was used. The CT images were independently assessed by two experienced radiologists who categorized the fibroids based on size, anatomical location (submucosal, intramural, subserosal, and transmural), lesion margin (well-defined, lobulated, and irregular), and calcification pattern. Calcification patterns were divided into non-coarse (punctate and amorphous) and coarse (peripheral, dense, and popcorn) patterns. Categorical variables were analyzed using the Chi-square and Fisher's exact tests, while continuous variables were evaluated using the Kruskal–Wallis test. Multivariate logistic regression analysis was conducted to determine the independent predictors of coarse calcifications. Statistical significance was set at $p < 0.05$.

Results

Amorphous calcifications accounted for 27.2% and peripheral calcifications for 23.8%, making them the most common patterns observed. There was a notable link between the pattern of calcification and its anatomical location ($\chi^2=14.97$, $p = 0.002$; Fisher's exact, $p = 0.001$). Coarse calcifications were predominantly found in intramural (45.6%) and transmural (10.3%) fibroids, whereas non-coarse patterns were more frequently observed in subserosal and submucosal areas. The size of the lesions varied significantly with different calcification patterns ($H = 11.02$, $p = 0.026$), with larger fibroids showing a tendency towards coarser calcification. No significant correlation was found between patient age and the calcification pattern ($p = 0.401$). In multivariate logistic regression, lesion size was identified as an independent predictor of coarse calcification (OR = 1.54, 95% CI: 1.06–2.22, P = 0.022). Lesions with irregular margins had lower odds of coarse calcification than those with well-defined margins (OR = 0.14, 95% CI: 0.03–0.69, P = 0.015).

Conclusion

The calcification patterns observed in uterine fibroids are significantly influenced by lesion size and anatomical location. Computed tomography (CT) imaging provides an effective means of characterizing

these patterns, potentially aiding clinical decision-making. Notably, larger intramural fibroids are more prone to coarse calcific degeneration.

Introduction

Uterine leiomyomas, also known as fibroids, are the most common benign tumors of the female reproductive system and are a major cause of gynecologic morbidity worldwide. These tumors originate from the smooth muscle cells of the myometrium and develop in 70–80% of women during their lifetime, with a higher prevalence observed among women of African descent [1, 2]. While many leiomyomas are asymptomatic, approximately one-third of affected women experience clinically significant symptoms, such as abnormal uterine bleeding, chronic pelvic pain, pelvic pressure, anemia, infertility, recurrent pregnancy loss, and urinary or bowel dysfunction. Consequently, uterine fibroids are among the primary reasons for hysterectomy and other gynecological interventions globally [3].

The clinical manifestations of uterine fibroids are significantly influenced by their size, quantity, and anatomical position. Intramural fibroids can disrupt uterine contractility and endometrial functions. Submucosal fibroids are frequently associated with heavy menstrual bleeding, infertility, and adverse reproductive outcomes. In contrast, subserosal fibroids typically cause compressive symptoms owing to their mass effect on adjacent pelvic structures [4]. Histopathologically, most fibroids are classified as typical leiomyomas, although several variants, such as cellular, lipoleiomyomatous, hydropic, and epithelioid types, have been identified [3].

Degenerative changes are common in uterine fibroids, particularly as these lesions enlarge and exceed their vascular supply. Calcification is regarded as a chronic, late-stage degenerative change predominantly observed in long-standing fibroids, especially among perimenopausal and postmenopausal women. The calcification process is thought to arise from ischemia, reduced blood flow, and progressive tissue degeneration within the leiomyoma, culminating in dystrophic calcium deposition [5, 6].

Calcified fibroids exhibit diverse morphological patterns, including peripheral rim-like, punctate, amorphous, coarse, dense, and popcorn calcifications. Identifying these patterns is clinically significant because calcified fibroids can mimic adnexal masses, pelvic stones, or malignant pelvic tumors on imaging studies [7]. While ultrasonography is the primary method for evaluating fibroids, computed tomography (CT) is highly sensitive in detecting calcium deposits and offers excellent characterization of the morphology, distribution, and extent of calcification [8].

Despite the acknowledged clinical importance of fibroid calcification, few studies have systematically investigated CT-based calcification patterns and their determinants, and no comprehensive studies have been conducted in Turkish populations. This study aimed to evaluate the spectrum and frequency of calcification patterns in uterine fibroids on CT and to determine their associations with patient age, lesion size, anatomical location, and lesion margin characteristics.

Methods

Study Design and Patient Population

This retrospective observational study was conducted at a tertiary care hospital after approval from the Institutional Review Board. Archived pelvic CT data and associated clinical records from January 2020 to December 2025 were systematically reviewed for this study. A non-probability consecutive sampling method was used to include all eligible pelvic CT examinations conducted during the study period. All CT scans were performed on 128- or 256-slice CT scanners, using standardized acquisition protocols.

Eligible patients were female, aged ≥ 30 years, with at least one histologically or radiologically confirmed uterine fibroid exhibiting calcification on CT, and with sufficient image quality to evaluate lesion size, margins, and anatomical location. The exclusion criteria were as follows: patients who had undergone prior uterine surgery, those with motion or imaging artifacts that precluded diagnostic interpretation, and those with incomplete clinical or radiological data. Cases with ambiguous calcification patterns or missing key variables (such as lesion size and calcification type) were also excluded to ensure consistency of the data.

A total of 140 patients met the eligibility criteria and were included in the final analyses.

Image Review and Data Collection

Two radiologists with substantial expertise in body imaging independently evaluated the computed tomography (CT) images. Each fibroid was analyzed based on the following parameters: maximum lesion diameter (measured in millimeters) across three orthogonal planes (anterior-posterior, transverse, and craniocaudal); lesion margin, categorized as well-defined, lobulated, or irregular; anatomical location, identified as submucosal, intramural, subserosal, or transmural; and calcification pattern. Discrepancies between the radiologists were resolved through discussion.

Calcification patterns were classified into five subtypes: punctate, amorphous, peripheral, dense, and popcorn. For analytical purposes, these subtypes were further grouped into two categories: non-coarse (punctate and amorphous) and coarse (peripheral, dense, and popcorn). Additionally, associated degenerative findings such as cystic changes, hemorrhage, or necrosis were documented when present.

Statistical Analysis

Data analysis was performed using SPSS version 20 (IBM Corp., Armonk, NY). Categorical variables were expressed as frequencies and percentages, and continuous variables were characterized by means and standard deviations. The chi-square test, or Fisher's exact test when expected cell counts were below five, was used to evaluate associations between categorical variables. The Kruskal–Wallis test was applied to compare continuous variables across the calcification groups, given their non-normal distribution. A multivariate logistic regression analysis was conducted to identify independent predictors

of coarse calcification, with lesion size, age, and margin characteristics as covariates. Statistical significance was set at $p < 0.05$.

Results

Patient and Lesion Characteristics

This study investigated 140 women diagnosed with calcified uterine fibroids, as confirmed by CT scans. The cohort primarily consisted of middle-aged to older individuals, with 29.9% aged 50–59, 25.2% aged 70–79, and 23.1% aged 60–69. A smaller segment (3.4%) was aged 30–39 years, and only 0.7% were 90 years or older. The majority of lesions were medium-sized, measuring between 21 and 40 mm (40.1%), followed by large lesions measuring 41–60 mm (21.8%) and small lesions measuring 20 mm or less (21.1%). Very large lesions measuring 61–80 mm and giant lesions exceeding 80 mm constituted 6.8% and 5.4% of the cases, respectively. Table 1 provides a detailed summary of the patient and lesion characteristics.

Regarding lesion morphology, well-defined margins were predominant, observed in 66.0% of cases, while irregular margins were present in 19.0% of cases, and lobulated margins in 10.2% of cases. The anatomical distribution of lesions was as follows: subserosal (37.4%), intramural (36.7%), submucosal (16.3%), and transmural (4.8%).

Among calcification patterns identified on CT, amorphous calcification was the most frequent (27.2%; Fig. 2**), followed by peripheral (23.8%;** Fig. 3**), punctate (21.8%;** Fig. 1**), popcorn (13.6%;** Fig. 5**), and dense (8.8%;** Fig. 4**) patterns.**.

Table 1
Patient and lesion characteristics (N = 140)

Variable	Frequency (N)	Percentage (%)
Age (years)		
30–39	5	3.4
40–49	14	9.5
50–59	44	29.9
60–69	34	23.1
70–79	37	25.2
80–89	5	3.4
≥90	1	0.7
Lesion size (maximum diameter)		
≤20 mm (small)	31	21.1
21–40 mm (medium)	59	40.1
41–60 mm (large)	32	21.8
61–80 mm (very large)	10	6.8
>80 mm (giant)	8	5.4
Lesion margin		
Well-defined	97	66.0
Lobulated	15	10.2
Irregular	28	19.0
Anatomical location		
Subserosal	55	37.4
Intramural	54	36.7
Submucosal	24	16.3
Transmural	7	4.8
Calcification pattern		
Amorphous	40	27.2
Peripheral	35	23.8
Punctate	32	21.8

Variable	Frequency (N)	Percentage (%)
Popcorn	20	13.6
Dense	13	8.8

Calcification Pattern and Anatomical Location

A statistically significant correlation was identified between the calcification pattern (coarse versus non-coarse) and the anatomical location of the lesion, as indicated by Pearson's $\chi^2(3) = 14.97$, $p = 0.002$, and Fisher's exact test $p = 0.001$. Non-coarse calcifications, characterized as punctate and amorphous, were predominantly found in subserosal (43.1%) and submucosal (25.0%) fibroids, with no occurrence in transmural lesions. In contrast, coarse calcifications, described as peripheral, dense, and popcorn-like, were most frequently observed in intramural lesions (45.6%) and were the sole pattern detected in transmural fibroids (10.3%). Table 2 provides complete cross-tabulation..

Table 2
Calcification pattern by anatomical location

Location	Non-coarse N (%)	Coarse N (%)	Total
Subserosal	31 (43.1%)	24 (35.3%)	55
Intramural	23 (31.9%)	31 (45.6%)	54
Submucosal	18 (25.0%)	6 (8.8%)	24
Transmural	0 (0.0%)	7 (10.3%)	7
Total	72 (100%)	68 (100%)	140

Pearson $\chi^2(3) = 14.97$, $p = 0.002$; Fisher's exact $p = 0.001$

Calcification Pattern and Lesion Margin

There was no statistically significant difference in the calcification pattern based on the lesion margin (Pearson’s $\chi^2(2) = 5.55$, $p = 0.062$; Fisher's exact $p = 0.063$). Well-defined margins were predominant in both the coarse (75.0%) and noncoarse (63.9%) groups. Non-coarse calcification was more frequently associated with lobulated margins (16.7%) than with coarse calcification (4.4%), whereas irregular margins were similarly distributed between the groups (19.4% vs. 20.6%). The comprehensive results are presented in Table 3.

Table 3
Calcification pattern by lesion margin

Margin	Non-coarse N (%)	Coarse N (%)	Total
Well-defined	46 (63.9%)	51 (75.0%)	97
Lobulated	12 (16.7%)	3 (4.4%)	15
Irregular	14 (19.4%)	14 (20.6%)	28
Total	72 (100%)	68 (100%)	140

Pearson $\chi^2(2) = 5.55$, $p = 0.062$; Fisher's exact $p = 0.063$

Calcification Pattern and Age

No statistically significant difference in patient age was identified among the five calcification subtypes, as indicated by the Kruskal–Wallis test ($H(4) = 4.04$, $p = 0.401$). The mean rank values were relatively similar across the groups: dense calcification exhibited the highest mean rank (82.15), followed by amorphous (73.54), punctate (73.39), and popcorn patterns (70.48). Peripheral calcification had the lowest mean rank (60.07). The findings are summarized in Table 4.

Table 4
Calcification pattern and patient age (Kruskal–Wallis test)

Calcification Pattern	N	Mean Rank
Amorphous	40	73.54
Peripheral	35	60.07
Punctate	32	73.39
Dense	13	82.15
Popcorn	20	70.48
Total	140	—

$H(4) = 4.04$, $p = 0.401$

Calcification Pattern and Lesion Size

A statistically significant variation in lesion size was observed among the five calcification subtypes (Kruskal–Wallis $H(4) = 11.02$, $p = 0.026$). Fibroids exhibiting popcorn calcification demonstrated the highest mean rank (83.28), followed by those with amorphous (77.55) and peripheral (71.81) patterns, suggesting an increase in lesion size within these groups. Conversely, punctate (63.13) and dense (43.77) calcification patterns were associated with smaller lesion sizes. These results imply that larger fibroids are more susceptible to coarse calcific degeneration. The results are presented in Table 5.

Table 5
Calcification pattern and lesion size (Kruskal–Wallis test)

Calcification Pattern	N	Mean Rank
Amorphous	40	77.55
Peripheral	35	71.81
Punctate	32	63.13
Dense	13	43.77
Popcorn	20	83.28
Total	140	—

H(4) = 11.02, p = 0.026

Multivariate Logistic Regression

The multivariate logistic regression model demonstrated statistical significance ($\chi^2(4) = 13.45$, $p = 0.009$), suggesting that the predictor variables effectively differentiated between coarse and non-coarse calcification patterns. The model exhibited an acceptable fit (Hosmer–Lemeshow $\chi^2(8) = 11.00$, $p = 0.201$), with an explained variance ranging from 9.2% to 12.2% (Cox & Snell $R^2=0.092$; Nagelkerke $R^2=0.122$).

Lesion size emerged as a significant independent predictor of coarse calcification (OR = 1.54, 95% CI: 1.06–2.22, p = 0.022), indicating that larger fibroids are significantly more prone to coarse calcification. Regarding lesion margin, the overall effect was significant (p = 0.031); specifically, irregular margins were associated with considerably lower odds of coarse calcification than well-defined margins (OR = 0.14, 95% CI: 0.03–0.69, p = 0.015), whereas lobulated margins did not achieve statistical significance (p = 0.857). Patient age was not identified as a significant predictor (p = 0.154). The regression coefficients are presented in Table 6.

Table 6
Multivariate logistic regression: predictors of coarse calcification

Variable	df	p-value	OR (Exp B)	95% CI Lower	95% CI Upper
Age	1	0.154	0.81	0.60	1.08
Lesion size	1	0.022	1.54	1.06	2.22
Margin (overall)	2	0.031	—	—	—
Lobulated vs. well-defined	1	0.857	0.92	0.39	2.21
Irregular vs. well-defined	1	0.015	0.14	0.03	0.69

Discussion

This retrospective study, based on computed tomography (CT), examined the range and determinants of calcification patterns in uterine fibroids in a Turkish cohort of 140 patients. The primary findings were as follows: (1) amorphous and peripheral calcifications were the most common patterns observed; (2) there was a significant association between calcification morphology and the anatomical location of the lesion, with coarse patterns predominantly found in intramural and transmural fibroids; (3) lesion size emerged as the sole significant independent predictor of coarse calcification; and (4) patient age did not significantly affect the calcification pattern. These results contribute population-specific data to a subject that is not fully characterized in the current literature and expand upon previous CT-based analyses of calcified fibroids [9, 10].

Calcification Patterns and Their Biological Significance

Calcification is a recognized late-stage degenerative change in uterine fibroids, occurring after ischemia, cellular necrosis, and extracellular matrix remodeling [5, 11]. Progressive vascular insufficiency within enlarging leiomyomas creates conditions conducive to dystrophic calcium deposition, which, unlike metastatic calcification, occurs despite normal systemic calcium metabolism [12]. The predominance of amorphous (Fig. 2) and peripheral(Fig. 3) patterns in the present study is consistent with published descriptions of fibroid calcification on CT, wherein peripheral rim calcification reflects gradual ischemic change beginning at the lesion margins, and amorphous deposition reflects more diffuse early stage mineralization [7, 10].

The association between coarse calcification and intramural/transmural locations is a novel finding. Intramural fibroids are the most deeply situated and typically have the most complex vascular architecture; a greater degree of fibrovascular involvement may predispose these lesions to more extensive and heterogeneous calcific degeneration. This interpretation is consistent with the observation that lesion size—but not age—independently predicted coarse calcification; larger fibroids, regardless of patient age, have a greater propensity to undergo advanced degeneration attributable to cumulative ischemic remodeling.

CT as the Optimal Modality for Calcification Assessment

Computed tomography (CT) remains the most sensitive imaging modality for the detection and classification of calcified pelvic lesions [8, 13]. Although ultrasonography is the primary method for evaluating fibroids, significant calcification can result in acoustic shadowing, which obscures the lesion margins and limits characterization [14]. Magnetic resonance imaging (MRI), renowned for its superior soft tissue resolution, is preferred for treatment planning; however, calcified regions appear as signal voids on both T1- and T2-weighted sequences, which hinders pattern analysis [15]. Consequently, CT provides a distinct advantage in characterizing calcification morphology in a reproducible and objective manner, which was utilized in the present study through systematic CT-based classification.

The clinical relevance of CT-based pattern classification was demonstrated by Crane et al. [9], who observed that coarse calcifications in untreated leiomyomas were consistently associated with MRI enhancement, indicating 100% viability, whereas diffuse and rim calcifications were predominantly nonviable. The distribution of patterns in the present cohort, with coarse patterns concentrated in deeper, larger lesions, supports the biological framework that coarse mineralization is linked to residual cellular activity rather than complete involutional changes. This distinction has practical implications for directing symptomatic patients toward appropriate interventions such as uterine artery embolization or myomectomy.

Age, Menopausal Status, and Calcification

The lack of a significant correlation between patient age and the calcification pattern observed in this study warrants further investigation. While calcification is conventionally associated with advancing age and postmenopausal estrogen withdrawal [16, 17], the current findings indicate that factors specific to the lesion, such as size and anatomical location, may exert a greater influence on calcification morphology than age. This observation is consistent with the prevailing understanding that leiomyomas constitute a biologically diverse group of tumors characterized by varying growth patterns and degenerative responses [18]. The predominance of cases within the 50–79-year age bracket (comprising 78.2% of the cohort) likely reflects the selection bias typical of retrospective CT-based studies of calcified fibroids.

Differential Diagnosis and Diagnostic Pitfalls

Accurate recognition of calcified uterine fibroids on CT is important to avoid misdiagnosis as ovarian neoplasms, urinary calculi, or pelvic phleboliths [7, 10]. Large subserosal calcified fibroids may mimic adnexal masses, particularly when pedunculated. Although extensive dystrophic calcification is a strong indicator of benign disease, it should not be considered pathognomonic, as rare cases of leiomyosarcoma with calcification have been reported [19]. Assessment of lesion margins, growth behavior, enhancement characteristics, and clinical context is essential when evaluating suspicious pelvic masses.

Strengths, Limitations, and Future Directions

The principal strengths of this study include its systematic CT-based methodology for classifying calcifications, the focus on a specific Turkish population that is underrepresented in the existing literature, the standardized image evaluation conducted by two experienced radiologists who reached a consensus, and the application of multivariable statistical analysis to identify independent imaging predictors.

This study has several significant limitations must be acknowledged. The retrospective single-center design limits the generalizability of the findings and introduces a potential selection bias. The relatively small sample size (n = 140) may have constrained the statistical power to detect subtle associations, particularly for less common calcification subtypes. Furthermore, histopathological confirmation was

not available for all lesions, precluding direct imaging-pathology correlations. Additionally, MRI data were unavailable in most cases, impeding the assessment of lesion viability, as described by Crane et al. [9]. Although a dual independent review with consensus was employed, inter-observer agreement statistics were not formally calculated.

Future multicenter prospective studies incorporating CT-based pattern analysis alongside multiparametric MRI, radiomics, and histopathological correlations are warranted. The integration of molecular imaging modalities, such as ^{18}F-NaF PET/CT, which has demonstrated uptake in calcifying leiomyomas and may distinguish metabolically active from end-stage calcification [20, 21], represents a promising avenue for further research. Artificial intelligence–based image analysis may enhance the automated classification and prediction of fibroid viability and treatment response.

In conclusion, the calcification patterns in uterine fibroids identified by CT imaging are significantly associated with lesion size and anatomical location. Larger, intramurally located fibroids are more likely to develop coarse calcific degeneration, while lesion size, rather than patient age, serves as the principal independent determinant. CT provides reliable characterization of these patterns and may contribute to clinical decision-making in the management of degenerative uterine fibroids.

Declarations

Ethics approval:

This retrospective chart review study was conducted in accordance with the ethical standards of the institutional and national research committee and the 1964 Helsinki Declaration and its later amendments.Approval was taken from Başakşehir Çam and Sakura City Hospital Istanbul, Turkey. The requirement for informed consent was waived by the ethics committee due to the retrospective nature of the study and the use of routinely collected clinical imaging data.

Competing interests:

The authors have no relevant financial or non-financial interests to disclose.

Consent for publication:

Not Applicable

Funding:

No funding was received for this study.

Author Contribution

All authors contributed to the study conception and design. V. H. and S. K. performed the data collection and image analysis. Statistical analyses were performed by G.K.S. and M.Y. The first draft of the manuscript was written by V.H., and all authors critically revised the subsequent versions. All the authors approved the final manuscript.

Data availability:

The datasets generated during the current study are available from the corresponding author upon reasonable request and subject to institutional data-sharing policies.

References

1. Giuliani E, As-Sanie S, Marsh EE. Epidemiology and management of uterine fibroids. Int J Gynaecol Obstet. 2020;149:3–9. https://doi.org/10.1002/ijgo.13102.
2. Bulun SE, Yin P, Wei J, et al. Uterine fibroids. Physiol Rev. 2025;105:1947–88. https://doi.org/10.1152/physrev.00010.2024.
3. Yang Q, Ciebiera M, Bariani MV, et al. Comprehensive review of uterine fibroids: developmental origin, pathogenesis, and treatment. Endocr Rev. 2021;43:678–719. https://doi.org/10.1210/endrev/bnab039.
4. Donnez J, Taylor HS, Marcellin L, Dolmans MM. Uterine fibroid-related infertility: mechanisms and management. Fertil Steril. 2024;122:31–9. https://doi.org/10.1016/j.fertnstert.2024.02.049.
5. Murase E, Siegelman ES, Outwater EK, et al. Uterine leiomyomas: histopathologic features, MR imaging findings, differential diagnosis, and treatment. Radiographics. 1999;19:1179–97. https://doi.org/10.1148/radiographics.19.5.g99se131179.
6. Koul A, Devi C, Bhagat I, et al. Calcification in uterine leiomyomas: pathophysiologic basis and imaging characteristics. Eur J Radiol. 2023;163:110812.
7. Wilde S, Scott-Barrett S. Radiological appearances of uterine fibroids. Clin Radiol. 2009;64:581–8. https://doi.org/10.1016/j.crad.2009.02.015.
8. Woźniak S, Woźniak A. CT imaging of pelvic calcifications: a systematic approach. Pol J Radiol. 2017;82:741–8.
9. Crane EP, Fenlon EP III, Ascher SM, et al. Evaluation of the viability of untreated leiomyomas using CT-detected calcification patterns. J Comput Assist Tomogr. 2021;46:57–63. https://doi.org/10.1097/RCT.0000000000001656.
10. Casillas J, Joseph RC, Guerra JJ. CT appearance of uterine leiomyomas. Radiographics. 1990;10:999–1007. https://doi.org/10.1148/radiographics.10.6.2259770.
11. Flake GP, Andersen J, Dixon D. Etiology and pathogenesis of uterine leiomyomas: a review. Environ Health Perspect. 2013;111:1037–54. https://doi.org/10.1289/ehp.5787.

12. Bazin D, Combes C, Rouzière S, et al. Absence of calcium phosphate compounds in dystrophic ossification of soft tissues. Clin Biochem. 2012;45:1001–6.
13. Tantipalakorn C, Khunamornpong S, Sukpan K, et al. Popcorn appearance of severely calcified uterine leiomyoma mimicking an adnexal mass. J Med Case Rep. 2023;17:312.
14. Bougie O, Warshafsky D, Dahan M. Ultrasound evaluation of uterine fibroids: practical guide. J Obstet Gynaecol Can. 2020;42:1060–8. https://doi.org/10.1016/j.jogc.2020.01.011.
15. Huch RA, Kunzi W, Debatin JF, et al. MR imaging of the non-gravid uterus. Eur Radiol. 2018;8:1323–35.
16. Flake GP, Moore AB, Sutton D, et al. The natural history of uterine leiomyomas: morphometric concordance with concepts of intermediary fibroblast differentiation. Fertil Steril. 2002;78:753–63. https://doi.org/10.1016/s0015-0282(02)03314-x.
17. Ulin M, Ali M, Chaudhry ZT, et al. Uterine fibroids in menopause and perimenopause. Menopause. 2019;27:238–42. https://doi.org/10.1097/GME.0000000000001438.
18. Koltsova AS, Bogomazova AN, Lagarkova MA. Uterine leiomyoma: known facts, common misconceptions. Int J Mol Sci. 2023;24:4728. https://doi.org/10.3390/ijms24054728.
19. Bush CH, Reith JD, Neff JR. Mineralization in musculoskeletal leiomyosarcoma: radiologic-pathologic correlation. AJR Am J Roentgenol. 2003;180:109–13.
20. Al-Zaghal A, Alenezi S, Werner T, et al. Incidental 18F-NaF uptake in a calcified uterine leiomyoma. Clin Nucl Med. 2018;43:e346–8. https://doi.org/10.1097/RLU.0000000000002224.
21. Resto DA, Park J, Choi HJ, et al. Monitoring the progression of a calcifying uterine leiomyoma with serial 18F-NaF PET/CT. Clin Nucl Med. 2022;47:e623–6. https://doi.org/10.1097/RLU.0000000000004266 / /.

Figures

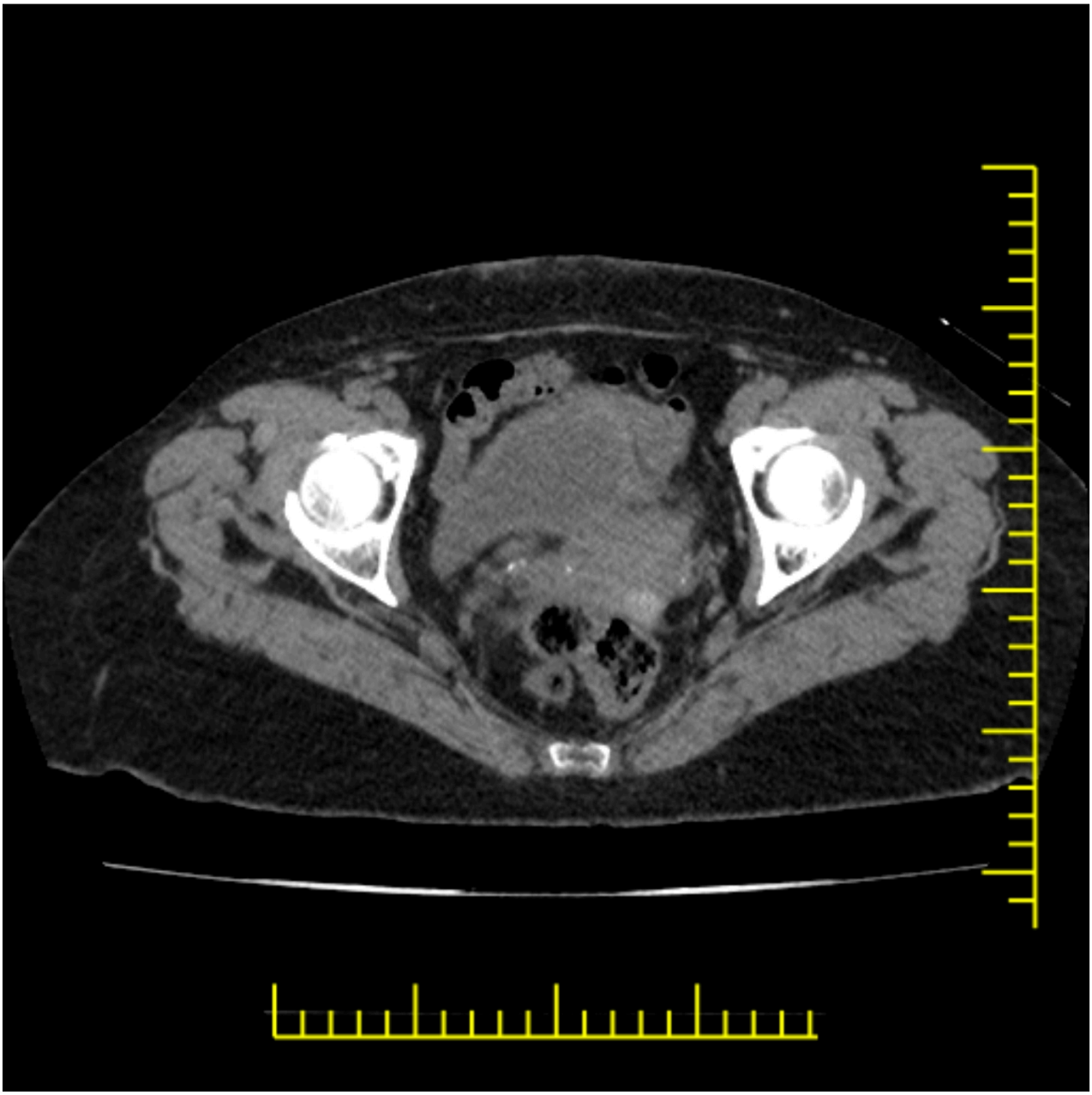


Figure 1

Punctate calcification pattern in a uterine fibroid (white arrowheads). Axial noncontrast-enhanced CT image shows multiple small, discrete, dot-like calcific foci scattered throughout the lesion parenchyma.

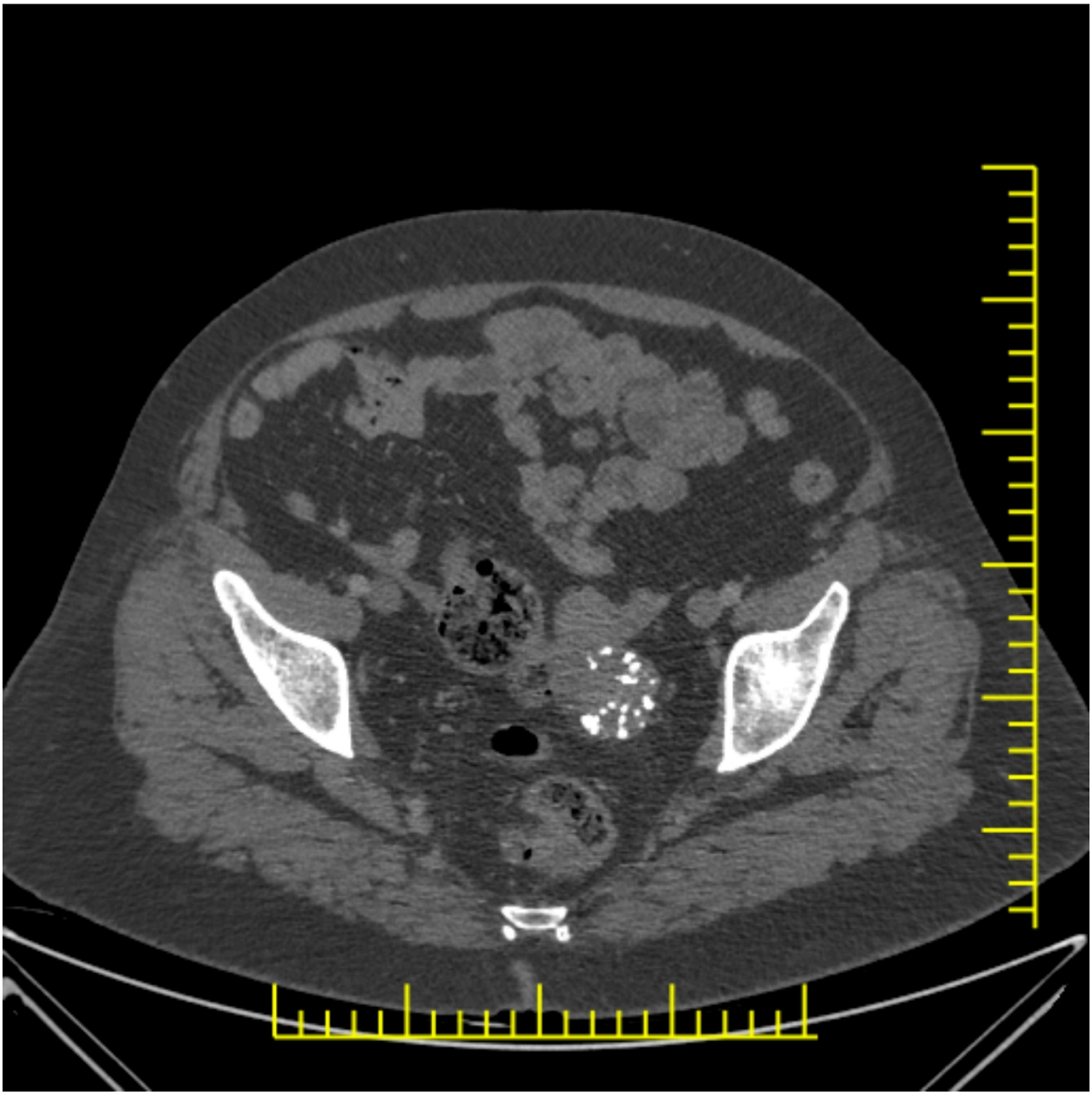


Figure 2

Amorphous calcification pattern in a uterine fibroid (white arrowheads). The axial CT image shows irregular, cloud-like, non-specific areas of calcium deposition without a clearly defined morphological configuration, consistent with early diffuse dystrophic mineralization

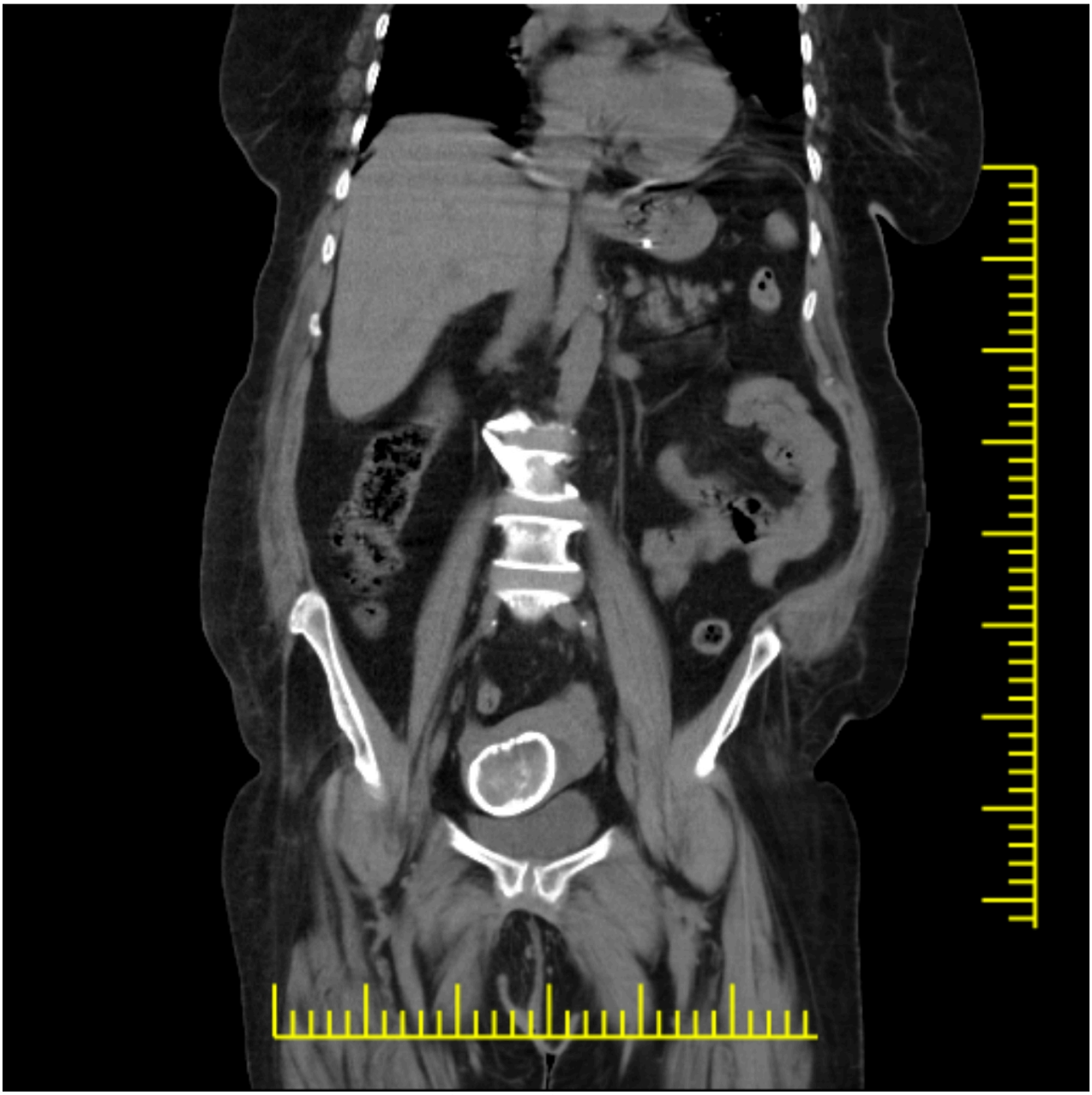


Figure 3

Peripheral (rim) calcification pattern in a uterine fibroid. Axial CT image demonstrates a curvilinear shell of calcium delineating the outer margin of the fibroid, reflecting ischemic change at the lesion's periphery.

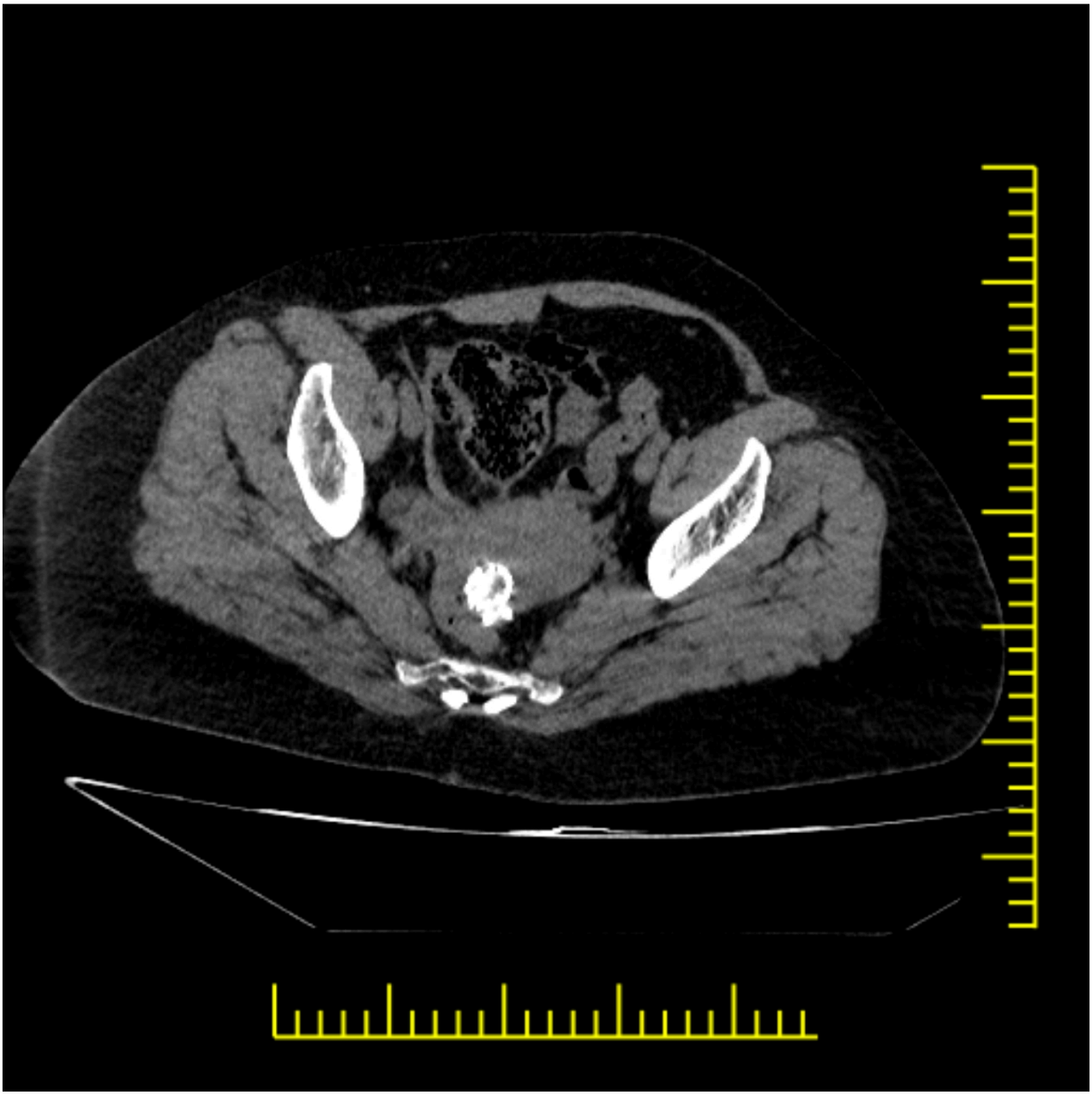


Figure 4

Dense (solid) calcification pattern in a uterine fibroid. Axial CT images show near-complete or extensive homogeneous calcification occupying the bulk of the fibroid, indicating advanced-stage end-organ mineralization.

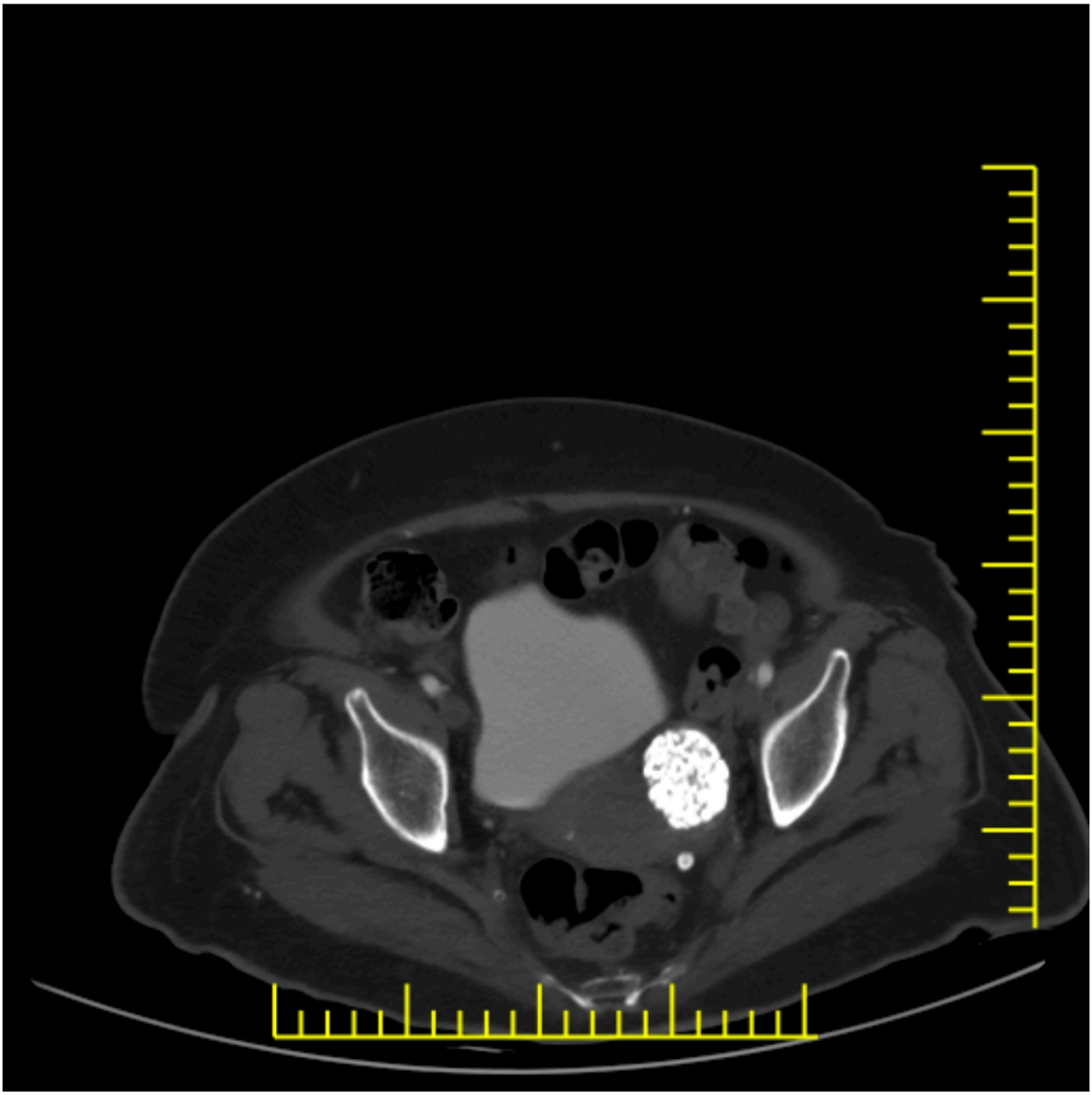


Figure 5

Popcorn calcification pattern in a uterine fibroid (white arrowheads). Axial CT image demonstrates multiple large, coarse, lobulated calcific nodules producing a characteristic “popcorn” appearance, typically associated with severely degenerated and/or previously treated leiomyomas.